



# Natural speckle-based watermarking with random-like illuminated decoding

XINKAI SUN,<sup>1,2</sup> SANGUO ZHANG,<sup>1,3</sup> RUI MA,<sup>4</sup> YE TAO,<sup>2,5</sup> YUPENG ZHU,<sup>2,5</sup> DONGYU YANG,<sup>2,5</sup> AND YISHI SHI<sup>2,5,\*</sup>

<sup>1</sup>School of Mathematical Sciences, University of Chinese Academy of Sciences, Beijing 100049, China

<sup>2</sup>Center for Materials Science and Optoelectronics Engineering, University of Chinese Academy of Sciences, Beijing 100049, China

<sup>3</sup>Key Laboratory of Big Data Mining and Knowledge Management, Chinese Academy of Sciences, Beijing 100190, China

<sup>4</sup>School of Electronics Engineering and Computer Science, Peking University, Beijing 100871, China

<sup>5</sup>School of Optoelectronics, University of Chinese Academy of Sciences, Beijing 100049, China

\*[optsys@gmail.com](mailto:optsys@gmail.com)

**Abstract:** We propose an optical watermarking method based on a natural speckle pattern. In the watermarking process, the watermark information is embedded into the natural speckle pattern. Then the random-like watermarked image is generated with the proposed grayscale reordering algorithm. During the extraction procedure, the watermarked image is projected to the natural speckle pattern as illumination. Subsequently, they are incoherently superimposed to extract the watermark information directly by human vision. Optical experiments and a hypothesis test are conducted to demonstrate the proposed method with high reliability, imperceptibility and robustness. The proposed method is the first watermarking method utilizing the natural diffuser as the core element in encoding and decoding.

© 2020 Optical Society of America under the terms of the [OSA Open Access Publishing Agreement](#)

## 1. Introduction

With the rapid development of information technology, information security is being taken seriously by more and more researchers, where optical watermarking technology plays an important role for its unique forms. In optical image watermarking, the original watermark is usually encoded by optical systems with high parallelism and speed. Then the optical ciphertext is embedded into the host image [1], and the embedded result is usually recorded on a physical medium. Optical watermarking with double random-phase encoding [2] innovated the form to process watermark image with optical system. In the following study, researchers extended the Fourier transform to a fractional Fourier transform [3,4] and expanded the 4f system to a general diffraction imaging system, i.e., the Fourier domain to the Fresnel domain [5,6]. Apart from 4f system, researchers also obtained a series of distinctive watermarking methods based on holography system [7–10], ghost imaging system [11,12], ptychography [13–15], single-pixel imaging system [16], etc. To improve the performance of the optical watermarking, researchers also take reference of advantages of other information encoding methods, such as visual cryptography (VC) [16–21], threshold secret sharing scheme [22–25], QR codes [15], etc.

In previous works, we have proposed several invisible visual cryptography (IVC) schemes. Different to the usual form, these schemes first disperse the watermark into multiple visual keys with VC [17–20]. Then optical elements are processed to record visual keys, which are parallel to optical ciphertext in the usual form of optical watermarking. In these works, it is inevitable to process optical elements. Hence, the watermarking technology is limited by the cost and precision of the process. To break the limitation of the optical elements process, one possible optimization solution is to replace processing components with natural materials, which not only reduces costs but also further increases security by utilizing unique natural materials as

physical keys. Coherent light through the diffuser body will produce natural speckle [26,27], and the intensity of speckle is of high complexity. When information is inserted to the speckle appropriately, it is difficult to detect and gather the inserted information without permission. Therefore, the speckle pattern is the natural host to embed the watermark.

In this paper, we propose a natural speckle-based watermarking with random-like illuminated decoding (NSWR). In watermarking procedure, the natural speckle pattern is generated with the optical system, and the watermark is inserted to the speckle pattern with the proposed grayscale reordering algorithm (GRA). The host with watermark, which is the output of GRA, is speckle-like with high imperceptibility. In extraction procedure, the watermarked image is projected to the host with a projector. Therefore, the watermarked is thought as random-like illumination. In NSWR, the original speckle pattern is indispensable to extract in extraction of the watermark. From the aspect of extraction, the watermark information is dispersed into two parts, one of which is natural speckle pattern generated from the natural diffuser and the other is artificial speckle pattern. Furthermore, decentralized information storage improves security of NSWR. To illustrate the imperceptibility of the random illumination, we introduce the ANOVA model [28] to fit the random illumination and construct a hypothesis test [29] based on ANOVA, which confirms the imperceptibility of our method at a given significance level (0.05).

## 2. Methodology

### 2.1. Procedure of extraction and watermarking

In many optical watermarking methods, the artificial optical device is the core component [17–19] which records the host with watermark. However, the artificial elements processing is often costly and the precision of elements is limited by the processing technology. To avoid these limitations, we use natural diffuser to replace the processed optical element as the key element and propose a natural speckle-based watermarking with random-like illuminated decoding (NSWR). Extraction procedure of NSWR is shown in Fig. 1, where two patterns from optical system and projector are stacked in the reflective surface.

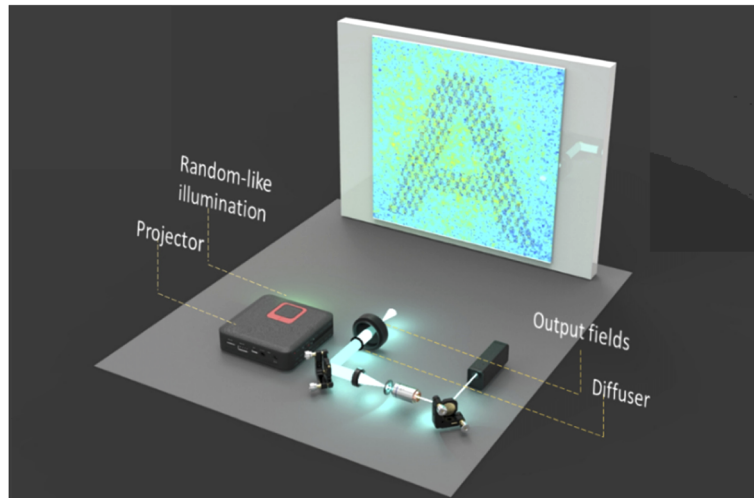


**Fig. 1.** The optical extraction of NSWR is based on the designed random-like illumination, which is generated from the projector.

In Fig. 1, the right side represents the generation of natural speckle pattern  $K$ . Specifically, the laser beam passes through the unique natural diffuser, and the output field is

$$U(x, y) = Am(x, y) \exp(j\varphi(x, y)), \quad (1)$$

where  $j = \sqrt{-1}$ . For the scattering effect of diffuser, the distribution of  $Am(x, y)$  and  $\varphi(x, y)$  are both with high complexity and strong randomness, and the distribution of  $U(x, y)$  is complicated. Then, the output fields generate speckle pattern  $K$  through the free-space propagation on the reflective surface.  $K$  can be presented as

$$K(x, y) = \left| \frac{e^{ikd}}{j\lambda d} \iint U(x_0, y_0) e^{\left[ \frac{jk}{2d} [(x-x_0)^2 + (y-y_0)^2] \right]} dx_0 dy_0 \right|^2, \quad (2)$$

where  $\lambda$  is the wavelength,  $k = 2\pi/\lambda$  is the wave vector, and  $d$  is Fresnel diffraction distance. For  $U(x, y)$  is complicated,  $K$  is also intricate. Moreover,  $K$  is vital for our method and is determined by the diffuser and parameters of the optical system. Apart from  $K$ , the designed random-like illumination  $C$  is another vital factor in extraction, which is projected to the same reflective surface in the left side of Fig. 1. Then, the superposition of the speckle pattern  $K$  and the illumination pattern  $C$  is extracted watermark, which is directly obtained by the human visual system. Although the speckle pattern is generated with coherent light, the extraction only requires incoherent superposition of two patterns. The only requirement is to stack  $K$  and  $C$ . Therefore, the extraction is convenient even for the users without any knowledge about optical watermarking.

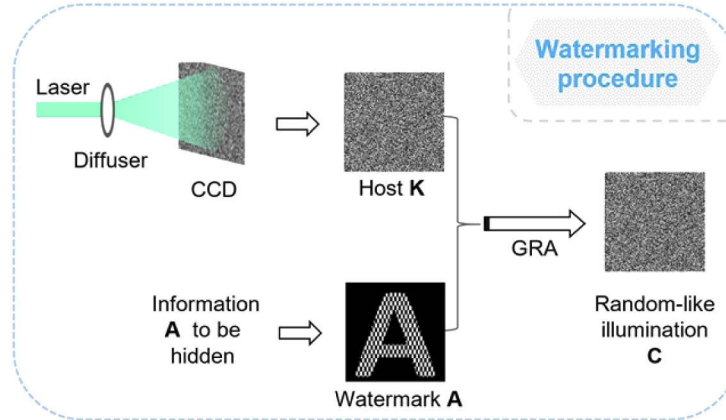


**Fig. 2.** The watermarking procedure of NSWR. In this procedure, a natural speckle pattern is used to generate a speckle-like key, which does not contain any clues of original information.

Corresponding to the extraction procedure described above, the framework of watermarking is shown in Fig. 2. In watermarking,  $K$  is the host, whose generation is shown in the top branch of Fig. 2. In the generation procedure of  $K$ , the optical system is equal to optical system in extraction, and the two optical system compare parameters and the same diffuser to generate the same speckle pattern. To embed the watermark, the  $K$  is recorded by a CCD, whose place is a reflective surface in extraction. In the bottom branch of Fig. 2, we suppose “A” is the watermark. To be suitable for the subsequent algorithm, “A” is visualized as a binary image  $A$ . As is shown in Fig. 2, the area displaying “A” in the binary image is white, while other area is dyed with black. Then the white area is filled with mosaic to add texture information and improve complexity. The original speckle pattern  $K$  and the watermark  $A$  are input to the grayscale reordering algorithm (GRA), the output of which is random-like pattern  $C$ . In fact,  $C$  is the watermarked image, which is rejected to the reflective surface as designed illumination in

extraction. Furthermore,  $C$  is generated via a speckle pattern and sustains the primary statistical property of the speckle pattern. It is difficult to find any clues of the watermark information, which means high imperceptibility. In NSWR, the watermark information is dispersed into  $K$  and  $C$ , for  $K$  and  $C$  are both indispensable in extraction. Furthermore,  $K$  is generated from the natural diffuser, which is the unique and unduplicated core component. Hence, our method is with high security, although the watermarked host is saved in digital.

## 2.2. Grayscale reordering algorithm

In watermarking process, the watermark is to inserted into the host with Grayscale Reordering Algorithm (GRA), the diagram of which is shown in Fig. 3. Inspired by visual cryptography (VC) [21], the purpose of GRA is to generate pattern carrying the watermark imperceptibly and reliably. Different from visual cryptography, the output of GRA is only the designed illumination  $C$ , while the input of the algorithm contains the watermark  $A$  and the natural speckle pattern  $K$ .

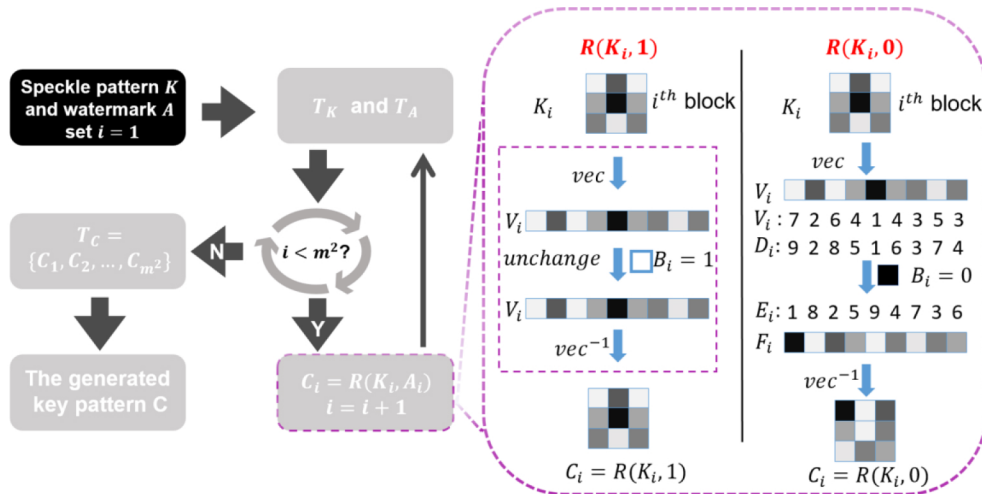


**Fig. 3.** The algorithm flow of GRA. The left side of the figure presents a framework of the algorithm, and the right side shows the operation of  $R(\cdot)$ .

In GRA, every pixel of binary image is parallelism to a block of the speckle pattern. Suppose the number of pixels in the binary image pattern  $A$  and the speckle pattern  $K$  is  $m \times m$  and  $km \times km$ , where  $k$  is a positive integer and  $k > 1$ . The speckle pattern  $K$  is divided into  $m^2$  blocks; every block contains  $k^2$  connected pixels; and the segmentation products a sequence with  $m^2$  elements  $T_K = \{K_1, K_2, \dots, K_{m^2}\}$ , which means the size of every  $K_i$  is  $k \times k$ . Accordingly, the watermark picture  $A$  is divided into a sequence with  $m^2$  elements by pixel to get  $T_A = \{A_1, A_2, \dots, A_{m^2}\}$ . Each element in  $T_A$  corresponds to the element in  $T_K$  which denotes every block corresponds to a pixel in the same location of the watermark. The element in  $T_K$  is the minimum unit in GRA, and every block will be operated differently depending on the corresponding element in  $T_A$ . Let  $C$  denotes the target illumination with same size of  $K$ , and segment  $C$  in the same way to get  $T_C = \{C_1, C_2, \dots, C_{m^2}\}$ .  $C_i$  is determined by  $K_i$  and  $A_i$ , hence block processing function  $R(\cdot)$  is introduced, and we have  $C_i = R(K_i, A_i)$ . With  $R(\cdot)$ , we build a framework of the algorithm which is shown on the left side of Fig. 3. Based on the above description, the GRA can be executed as follows

**Step1** Input the speckle pattern  $K$  with  $km \times km$  size and plaintext pattern  $A$  with  $m \times m$  size; Set  $i = 1$ ;

**Step2** Produce sequence  $T_K$  and  $T_A$  with segmentation of  $K$  and  $A$ ;

**Step3** If  $i < m^2$ , execute **Step4**, otherwise execute **Step5**;

**Step4** Calculate  $C_i = R(K_i, A_i)$ , which is defined above, and more detail is shown in the bottom of Fig. 3;  $i = i + 1$ ; Execute **Step3**

**Step5** Output  $T_C$  and obtain  $C$

The left side of Fig. 3 presents the details of  $R(\cdot)$ . As mentioned earlier, the operation of each block is connected to the corresponding pixel. For every block, there are 3 steps to generate a processed block. To illuminate the procedure, we suppose that all blocks contain  $3 \times 3$  pixels. The definition of  $R(\cdot)$  is shown on the right side of Fig. 3. The value of  $A_i$  determines that of  $R(K_i, A_i)$ :  $A_i = 1, R(K_i, A_i) = R(K_i, 1) = K_i$ ;  $A_i = 0$ , the operation of  $R(K_i, 0)$  is pretty complexed which is explained as follow. Firstly,  $K_i$  is straightened into a  $k^2$ -dimension vector, which is recorded as  $V_i = \text{vec}(K_i)$ . Note that, straightening operation is reversible when the scale of  $K_i$  is known and there is a function  $\text{vec}^{-1}$  satisfying  $K_i = \text{vec}^{-1}(V_i)$ . Secondly, let  $D_i$  denote the rank sequence of  $V_i$ ,  $D_{ij} = \sum_{t=1}^{k^2} I_{\{V_{ij} \geq V_{it}\}}(V_{ij})$ , where  $I_{\{V_{ij} \geq V_{it}\}}$  is an indicative function.  $I_{\{V_{ij} \geq V_{it}\}}(V_{ij}) = 1$ , if and only if  $V_{ij} \geq V_{it}$ . Otherwise,  $I_{\{V_{ij} \geq V_{it}\}}(V_{ij}) = 0$ . For example, suppose  $V_i = (4, 2, 3)$ , then  $D_i = (3, 1, 2)$ , which is for  $2 < 3 < 4$  in  $V_i$ , and the order of 4,2,3 is 3,1,2, respectively.

If there are equal components in  $V_i$ , the same with  $D_i$ . In this case, we need to correct  $D_i$ , adjust the repeated elements in  $D_i$  down to integers not included in  $D_i$ , and finally make the elements in  $D_i$  include all integers between 1 and  $k^2$ . Thirdly, take the complement of  $k^2 + 1$  for each element in  $D_i$  and get the complement sequence  $E_i$  and  $E_{ij} = k^2 + 1 - D_{ij}$ . The elements of  $V_i$  are rearranged according to  $E_i$  to obtain the rearrangement sequence  $F_i$ .  $F_i$  contains the same element as  $V_i$ , but its rank sequence is  $E_i$ . For example,  $V_i = (4, 2, 3)$ , then  $D_i = (3, 1, 2)$ ,  $E_i = (1, 3, 2)$ ,  $F_i = (2, 4, 3)$ . Finally,  $F_i$  is folded into a matrix with the same scale as  $K_i$  and to produce  $C_i = R(K_i, 0) = \text{vec}^{-1}(F_i)$ . Corresponding to the original image, the blocks connected with white pixel will stay the same, while other blocks will get significant adjustment. All block will be processed and the processed blocks are arranged in corresponding order to compose the key pattern.

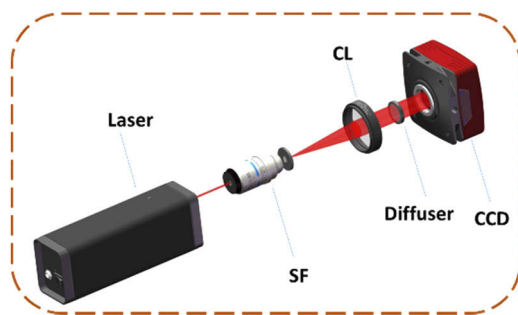
The adjustment from  $R(\cdot)$  is vital for extraction. Specifically, the blocks with opposite order are stacked to show more uniform grayscale values. Hence, the superimposition result of original blocks has a different visual effect compared to the superimposition of original and adjusted blocks. Different visual effect is distinguished by human visual system, and the extracted information is obtained.

### 3. Experimental results and basic analysis

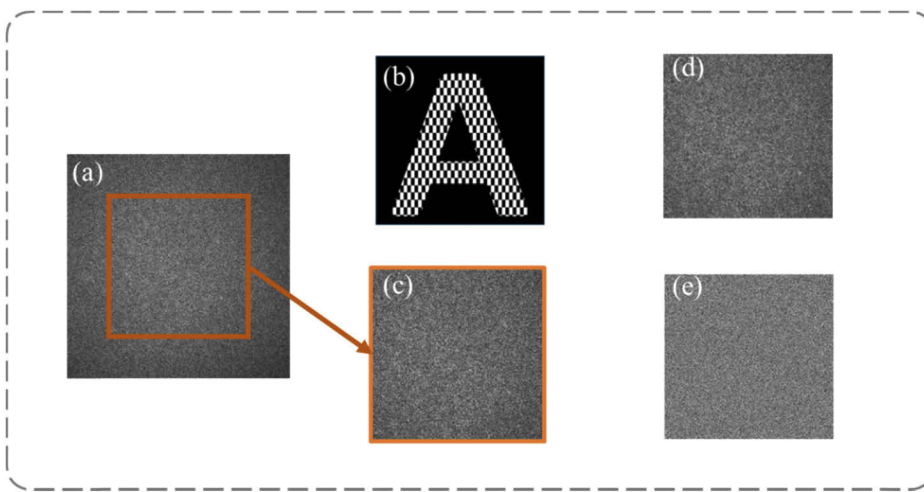
#### 3.1. Results of watermarking

We have performed optical experiments to demonstrate our method. The watermarking results are shown in Fig. 5. We still regard ‘A’ as the information to be hidden. In the watermarking process, with procedure described as above, ‘A’ is visualized as a binary image filled with mosaic shown as Fig. 5(b). The image of visualized ‘A’ contains  $128 \times 128$  pixels. Figure 4 gives an optical setup to gain intensity distribution of speckle. We use a laser source (THORLABS, HNL-S008R, 632.8nm), a spatial filter (SF) with the collimating lens (CL)( $f = 75\text{mm}$ ), which consists of a microscope objective lens (40x, 0.65NA) and a pinhole aperture ( $D = 10\mu\text{m}$ ), to generate a collimated beam. After being collimated, the beam passes through the diffuser (THORLABS, DG10-600-A, grit=600). Then the Fresnel diffraction pattern formed by the light is recorded on the charge coupled device (CCD) (Mikrotron, EoSens, pixel size= $8\mu\text{m}$ ) camera. Finally, we gain the intensity distribution of speckle shown in Fig. 5(a).

There are  $1024 \times 1024$  pixels in the speckle pattern collected with CCD, and the area is selected as the input speckle of the algorithm. As shown in Fig. 5(c), we only cut out a subset with  $640 \times 640$  pixels from the speckle pattern. After that, the watermark image 5(b) and the cropped



**Fig. 4.** The experimental setup to generate the speckle pattern. To embed the watermark, the speckle pattern is recorded by CCD.



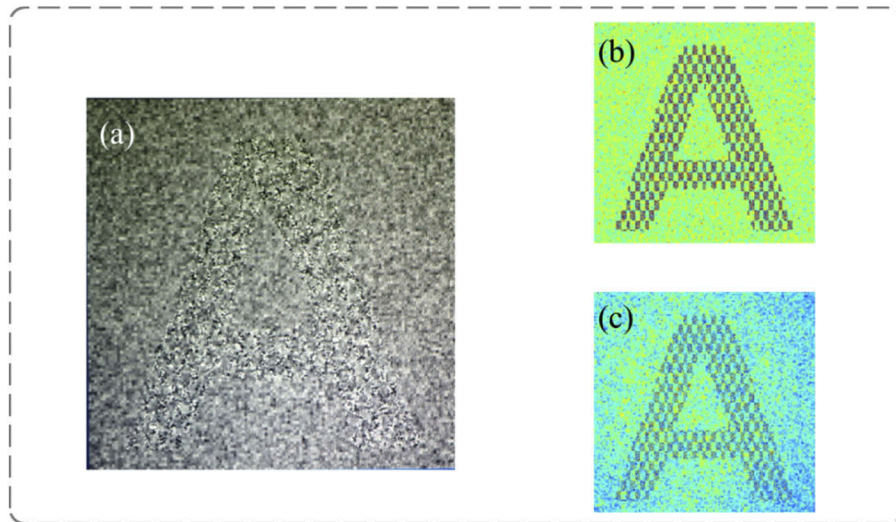
**Fig. 5.** Related pictures of watermarking. (a) is the speckle pattern obtained by CCD, and (c) is the subset of (a). (b) is the target picture embedded to the host. (d) and (e) are watermarking results. (d) is the output of GRA with the host of (c), while the corresponding host is a simulated speckle pattern.

image are input to GRA. In GRA, the speckle pattern is divided into  $128 \times 128$  blocks with same size, which means every pixel in watermark image is expanded  $5 \times 5$  pixels. Figure 5(d) presents the generated random-like illumination pattern of  $640 \times 640$  pixels, which is the output of GRA, and Fig. 5(e) is the illumination pattern from a simulated speckle pattern. As shown in Figs. 5(d) and 5(e), there is no clues of 'A' in generated patterns. The result of hiding simply shows the feasibility and security of our methodology.

### 3.2. Results of extraction

As is mentioned above, the optical extraction process is based on incoherent superposition. Concretely, the wave front carrying the host information and random-like illumination are superimposed on the reflective surface. Then the watermark will appear. The main obstacle is that two wave fronts need to be stacked. In experiment, the collected speckle pattern is limited to the size of CCD with only a few square centimeters, while ordinary projectors project images of sizes typically in the range of a few square meters. Aligning two patterns with such divergence is not easy with ordinary optical experimental devices. However, in this article, all our efforts are put to prove some basic properties of our methodology such as feasibility, imperceptibility,

security and robustness rather than developing a highly reliable hardware system. Hence, an equivalence experiment is necessary. A viable alternative is to use a projector to project the natural speckle pattern onto a reflective surface, too. For matching the wave front, we use a projector to reproduce the two patterns without changing the verification effectiveness of the experiment. In the specific experiment, we do not change the position of the projector and the screen. Then we use the projector to output two wave fronts. In view of subsequent operations, images on the screen are recorded respectively with a camera in the same position. Finally, the superposition process is simulated and the images recorded by the camera are synthesized in the computer to obtain the final result of optical extraction. Extraction results are shown in Fig. 6. Figure 6(a) is the result of equivalent optical extraction experiment with Canon EOS 90D camera with EFS 18-135 mm lens regaining the speckle patterns, the dynamic range and contrast of which are adjusted simply. For the equivalent experiment brings noise and disturbances inevitably, the extraction result is distorted slightly. Figures 6(b) and 6(c) shows the simulated extraction result with pseudo-color for better visual effects. Figure 6(b) is the superposition of Fig. 5(e) and corresponding speckle pattern, and Fig. 6(c) is superposition of Fig. 5(c) and Fig. 5(d) via computer software without optical reproduction.



**Fig. 6.** Related pictures of the extraction procedure. (a) is the result of equivalent optical extraction experiment. (b) and (c) are both simulated extraction results. The corresponding host of (a) is the simulated speckle pattern, while the hosts of (c) is Fig. 5(c), (a) real speckle pattern

### 3.3. Basic analysis

This section contains some intuitive and basic analyses of NSWR based on the experiment and simulation results.

Firstly, as is shown in Figs. 6(a) and 6(c), the random-like illumination generated by the GRA obtains the relevant information of the original picture. In Figs. 6(a) and 6(c), the boundary of the between black and white area is the outline of “A”, hence superposition image reflects the basically relevant information of the original image. Subject to the algorithm itself, the extraction result loses partial contrast compared with the original image, but these losses do not affect the acquisition and extraction of relevant information. This further confirms the feasibility of our method in both simulation and laboratory.

Secondly, let's visually illustrate the security of our method. Figures 5(c) and 5(d) are highly similar, and distributions of their pixel values present strong randomness in space. Then comparing Figs. 5(d) with 6(a) or 6(c), distinct border of black and white pixel does not appear in Fig. 5(d). It is reasonable to assume that the generated illumination pattern does not contain any valid information. These analyses initially confirm that our method possesses with high imperceptibility, which directly shows high security.

#### 4. Imperceptibility and robustness analysis

##### 4.1. Hypothesis testing and imperceptibility

As imperceptibility is prior in watermarking, we use hypothesis test as a tool to conduct a more detailed quantitative analysis in this section. Hypothesis test is a tool to judge whether a proposition is true or false in the view of statistics. Hypothesis test can not only make a judgment according to the data, but also evaluate the reliability of the conclusion to control the risk of making mistakes. Therefore, it has considerable reliability. Assumed the null hypothesis  $H_0$  and the alternative hypothesis  $H_1$  are given, the first step of hypothesis test is to form the test statistic, which will distinguish  $H_0$  and  $H_1$ . Then, the probability distribution of the statistic is deduced under  $H_0$  and the observation of test statistic can be obtained using sample data. Finally,  $p$ -value is calculated according to the observation under zero distribution and compared with the given threshold to make decision [29]. In this section, we use hypothesis test to make quantitative and accurate analysis of the imperceptibility of our watermarking method following the steps mentioned above.

Initially, we determine the null hypothesis  $H_0$  and alternative hypothesis  $H_1$ , which represent imperceptibility of illumination pattern. In illumination pattern, imperceptibility means that the hidden information can't be obtain by the human's visual system directly. Human's visual system distinguishes information from spatial stratification of images. For the illumination pattern, spatial stratification means difference of pixels' gray values in different areas. Once there is no significant distinction among areas of the illumination patterns, it is reasonable to speculate high imperceptibility of our method. Based on above analysis, we proposed the null hypothesis  $H_0$  and alternative hypothesis  $H_1$  as:

$H_0$ : there is no spatial stratification in the illumination image;

$H_1$ : there is spatial stratification in the illumination image.

In order to construct the test statistic, we first divide the watermarked speckle pattern into  $s$  groups. The  $i$ -th group contains  $n_i$  connected pixels, where  $1 \leq i \leq s$ . We assume the intensity distribution of the natural speckle is Gaussian distribution  $N(\mu, \sigma^2)$ , for the Gaussian distribution helps to reduce difficulty of the hypothesis test and does not change the result. Furthermore, the shape of real distribution is similar to the Gaussian distribution, while the real distribution is complexity and partially unknown. It should be noted that only a part of pixels' position is adjusted in GRA. It is reasonable to suppose the illumination and speckle with similar distribution. However, some areas in the extraction result are with high intensity level, which means gray value level of some groups may be changed by GRA. Hence, we utilize ANOVA model [28] to fit the pixel's data of artificial speckle. Specifically, One-way ANOVA model decomposes pixel's gray value as  $X_{ij} = \mu_i + \epsilon_{ij}$ ,  $1 \leq i \leq s$ ,  $1 \leq j \leq N_i$ , where  $\mu_i$  is a constant presenting the average level of gray value in  $i$ -th group, and  $\epsilon_{ij}$  is independent random variable and satisfies  $N(0, \sigma^2)$ . Between-group and inter-group difference can be expressed as  $SSW = \sum_{i=1}^s \sum_{j=1}^{N_i} (x_{ij} - \bar{x}_i)^2$ ,  $SSB = \sum_{i=1}^s N_i (\bar{x}_i - \bar{x})^2$ , where  $\bar{x}_i = \frac{1}{N_i} \sum_{j=1}^{N_i} x_{ij}$ ,  $\bar{x} = \frac{1}{N} \sum_{i=1}^s \sum_{j=1}^{N_i} x_{ij}$ .  $SSW$  denotes the sum of each group's fluctuation level, and  $SSB$  denotes the sum of difference of average level among groups. Let  $SST = \sum_{i=1}^s \sum_{j=1}^{N_i} (x_{ij} - \bar{x})^2$ , then we have  $SST = SSW + SSB$ .

Furthermore,  $SST$  is a constant determined by the variance  $\sigma^2$ . When  $SSB$  is small and  $SSW$  is large, difference among groups is tiny and spatial stratification is not significant. Hence, we

construct the  $F$  – statistic as

$$F = \frac{SSB}{SSW}. \quad (3)$$

$F$  decreases with high imperceptibility. When  $x_{ij}$  is independent and follows normal distribution  $N(\mu_i, \sigma^2)$ , we have  $\frac{N-s}{s-1} F \sim F(N - s, s - 1)$ .

In fact, the size of patterns is  $640 \times 640$ , and the grey value of a pixel is integer values between  $0 \sim 255$ . Therefore, we assume that the original speckle image's grey value distribution is the binomial distribution  $B$  ( $255, 1/2$ ). According to central limit law, the binomial distribution  $B(255, 1/2)$  approximates the normal distribution  $N(255/2, 255/4)$ . The illumination pattern is divided several groups of  $50 \times 50$  pixels. To generate kinds of segmentations, we set the coordinate  $(m, n)$  to adjust the segmentation. As shown in Fig. 7,  $(m, n)$  is coordinate of the first pixel in the first group. Moreover, the segmentation strategy is changed with adjustment of  $(m, n)$ . For the offset parameters, there are some pixels not in any group. Here, we guarantee most of pixels selected, and the limited number of these pixels does not have a substantial impact on the hypothesis test. When  $(m, n)$  is set, the number of groups  $s$  and the number of pixels in groups are determined.

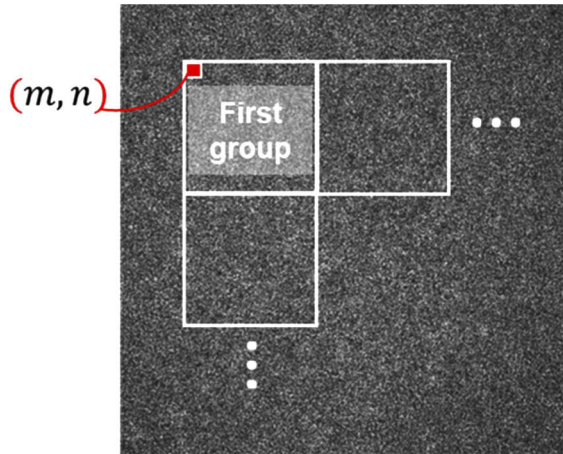


**Fig. 7.** Offset parameters for division strategy. The watermarked host is divided into a series of groups, and offset parameters are set to adjust the division strategy with size of groups unchanged.

The parameter settings and simulation results are shown in Table 1. The data set include 150 samples, all of which contain original speckle pattern, illumination pattern and the extraction result. The speckle pattern is independently generated from  $B(255, 1/2)$ , and the other two patterns are based on the speckle with watermark information of Fig. 5(b). To demonstrate imperceptibility sufficiently, we use two offsets (7, 8) and (13, 23) to generate two kind of segmentation. As for the procedure of testing, we firstly calculate the observations of  $F$  and  $\frac{N-s}{s-1} F$ , and obtain the  $p$ -value under the null distribution  $F(N - s, s - 1)$ . Finally, the  $p$ -value is compared with the threshold value (0.05). If the value is greater than the threshold, we accept  $H_0$ . Otherwise we reject the null hypothesis. Except the rejection number, other values are shown as average and deviation in brackets, while the  $p$  – value and rejection number for extraction pattern are not known for lack of distributions.

Furthermore, we calculate the observation based on the original speckle pattern and the extraction result, too. Moreover, we also record number of rejections. As shown in Table 1, there observations of statistics are close and the  $F$  – statistic is useless to distinguish the speckle pattern

**Table 1. Result of hypothesis testing**

Offset	Pattern	F	$\frac{N-s}{s-1} F$	p-value	Rej Num <sup>a</sup>
(7, 8)	Host with watermark	$4.01 \times 10^{-4}$ ( $5.25 \times 10^{-5}$ )	1.01 (0.13)	0.48 (0.26)	6
(7, 8)	Speckle	$3.64 \times 10^{-4}$ ( $4.66 \times 10^{-5}$ )	0.99 (0.12)	0.52 (0.29)	7
(7, 8)	Extraction result	$4.67 \times 10^{-4}$ ( $5.19 \times 10^{-5}$ )	1.17 (0.14)	—	—
(13, 23)	Host with watermark	$3.99 \times 10^{-4}$ ( $4.99 \times 10^{-5}$ )	0.99 (0.12)	0.51 (0.29)	6
(13, 23)	Speckle	$3.99 \times 10^{-4}$ ( $4.99 \times 10^{-5}$ )	1.00 (0.13)	0.50 (0.30)	5
(13, 23)	Extraction result	$4.65 \times 10^{-4}$ ( $5.50 \times 10^{-5}$ )	1.17 (0.14)	—	—

<sup>a</sup>Rej Num is the abbreviation of Rejection Number

and the host with watermark. From the aspect of hypothesis testing, the watermarked host is with imperceptibility equal to the host, while the extraction is clearly distinguished by *F – statistic*.

#### 4.2. Robustness analysis

For watermarking systems, some perturbations are unavoidable, and robustness is a key performance indicator to evaluate a system or method. Noise is a common form of interference in systems, i.e. a host image is mixed up with noise for various reasons. Taking Gaussian noise as an example, we add the noise to the illumination pattern, which is shown in Fig. 5(d) to get the noise-interfered illumination, and superimpose the noise-interfered illumination pattern to the speckle pattern in Fig. 5(c) to get the extraction image with noise. Extraction results with noise are shown in Fig. 8. All patterns are with  $640 \times 640$  pixels, and the pixel size is  $8 \mu\text{m}$ . In Fig. 8(a), the amplitude of noise is equal to the amplitude of the host with watermark. In Fig. 8(b), the amplitude of noise is 1.6 times of the amplitude of the host with watermark. In both two results, the outline of “A” can be distinguished, which means NSWR with high tolerance to noise.

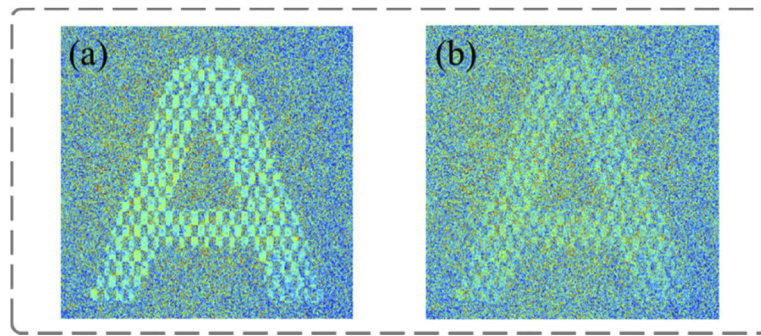


**Fig. 8.** Extraction results with noise attacking. (a) is with the amplitude of noise equal to the amplitude of the host, and the amplitude of noise in (b) is 1.6 times of the amplitude of the host with watermark.

#### 5. Conclusions

In this paper, we propose the natural speckle-based watermarking method, the extraction of which is based on random-like illumination. In watermarking, the watermark information is dispersed into the natural speckle pattern and the random-like illumination pattern. GRA is the core process of watermarking. Furthermore, GRA is also a digital watermarking method, which embeds a binary image watermark into a random-like host. In extraction, the watermark information is obtained by naked eyes with stacking the speckle pattern and the illumination

pattern. We also demonstrate NSWR is with high reliability and imperceptibility. Furthermore, NSWR is also with high robustness of defending noise.

## Funding

Natural Science Foundation of Beijing Municipality (Z190004); Key Program of Joint Funds of the National Natural Science Foundation of China (U19B2040); University of Chinese Academy of Sciences (Y95401TXX2); National Natural Science Foundation of China (61575197); Youth Innovation Promotion Association of the Chinese Academy of Sciences (2017489); Fusion Foundation of Research and Education of CAS; Natural Science Foundation of Hebei Province (F2018402285).

## Acknowledgments

The authors would like to thank Guilin Li and Tao Yu from OIIV Lab (UCAS) for discussions and assistance with this work.

## Disclosures

The authors declare no conflicts of interest.

## References

1. S. Jiao, C. Zhou, Y. Shi, W. Zou, and X. Li, "Review on optical image hiding and watermarking techniques," *Opt. Laser Technol.* **109**, 370–380 (2019).
2. P. Refregier and B. Javidi, "Optical image encryption based on input plane and Fourier plane random encoding," *Opt. Lett.* **20**(7), 767 (1995).
3. Y. Zhang, C.-H. Zheng, and N. Tanno, "Optical encryption based on iterative fractional Fourier transform," *Opt. Commun.* **202**(4-6), 277–285 (2002).
4. Z. Liu and S. Liu, "Double image encryption based on iterative fractional Fourier transform," *Opt. Commun.* **275**(2), 324–329 (2007).
5. Y. Shi, G. Situ, and J. Zhang, "Multiple-image hiding in the Fresnel domain," *Opt. Lett.* **32**(13), 1914 (2007).
6. X. Li, X. Meng, Y. Wang, X. Yang, Y. Yin, X. Peng, W. He, G. Dong, and H. Chen, "Secret shared multiple-image encryption based on row scanning compressive ghost imaging and phase retrieval in the Fresnel domain," *Opt. Lasers Eng.* **96**, 7–16 (2017).
7. N. K. Nishchal, J. Joseph, and K. Singh, "Fully phase encryption using digital holography," *Opt. Eng.* **43**(12), 2959–2967 (2004).
8. X. Wang, D. Zhao, and L. Chen, "Image encryption based on extended fractional Fourier transform and digital holography technique," *Opt. Commun.* **260**(2), 449–453 (2006).
9. D. Kong, L. Cao, X. Shen, H. Zhang, and G. Jin, "Image Encryption Based on Interleaved Computer-Generated Holograms," *IEEE Trans. Ind. Inform.* **14**(2), 673–678 (2018).
10. X. Li, Y. Wang, Q.-H. Wang, S.-T. Kim, and X. Zhou, "Copyright protection for holographic video using spatiotemporal consistent embedding strategy," *IEEE Trans. Ind. Inform.* **15**(11), 6187–6197 (2019).
11. P. Clemente, V. Durán, E. Tajahuerce, and J. Lancis, "Optical encryption based on computational ghost imaging," *Opt. Lett.* **35**(14), 2391–2393 (2010).
12. L.-J. Kong, Y. Li, S.-X. Qian, S.-M. Li, C. Tu, and H.-T. Wang, "Encryption of ghost imaging," *Phys. Rev. A* **88**(1), 013852 (2013).
13. Y. Shi, T. Li, Y. Wang, Q. Gao, S. Zhang, and H. Li, "Optical image encryption via ptychography," *Opt. Lett.* **38**(9), 1425 (2013).
14. W. Xu, H. Xu, Y. Luo, T. Li, and Y. Shi, "Optical watermarking based on single-shot-ptychography encoding," *Opt. Express* **24**(24), 27922 (2016).
15. Y. Zhu, W. Xu, and Y. Shi, "High-capacity encryption system based on single-shot-ptychography encoding and QR code," *Opt. Commun.* **435**, 426–432 (2019).
16. S. Jiao, J. Feng, Y. Gao, T. Lei, and X. Yuan, "Visual cryptography in single-pixel imaging," *Opt. Express* **28**(5), 7301 (2020).
17. Z. Li, G. Dong, D. Yang, G. Li, Y. Shi, K. Bi, and J. Zhou, "Efficient dielectric metasurface hologram for visual-cryptographic image hiding," *Opt. Express* **27**(14), 19212 (2019).
18. N. Yang, Q. Gao, and Y. Shi, "Visual-cryptographic image hiding with holographic optical elements," *Opt. Express* **26**(24), 31995 (2018).
19. Y. Shi and X. Yang, "Optical hiding with visual cryptography," *J. Opt.* **19**(11), 115703 (2017).
20. Y.-S. Shi and X.-B. Yang, "Invisible Visual Cryptography," *Chin. Phys. Lett.* **34**(11), 114204 (2017).

21. M. Naor and A. Shamir, "Visual cryptography," in *Advances in Cryptology — EUROCRYPT'94*, A. De Santis, ed. (Springer, Berlin Heidelberg, 1995), pp. 1–12.
22. X. Pan, X. Meng, Y. Wang, X. Yang, X. Peng, W. He, G. Dong, and H. Chen, "Multilevel image authentication using shared secret threshold and phase retrieval," *J. Mod. Opt.* **61**(18), 1470–1478 (2014).
23. X. Deng, W. Wen, X. Mi, and X. Long, "Optical threshold secret sharing scheme based on basic vector operations and coherence superposition," *Opt. Commun.* **341**, 22–27 (2015).
24. X. Deng, Z. Shi, and W. Wen, "Threshold secret sharing scheme based on phase-shifting interferometry," *Appl. Opt.* **55**(31), 8855 (2016).
25. X. Deng, W. Wen, and Z. Shi, "Threshold multi-secret sharing scheme based on phase-shifting interferometry," *Opt. Commun.* **387**, 409–414 (2017).
26. J. W. Goodman, *Statistical Optics*, Wiley classics library ed, Wiley Classics Library (Wiley, 2000).
27. J. W. Goodman, *Speckle Phenomena in Optics: Theory and Applications* (Roberts and Company Publishers, 2007).
28. J. Shao, *Mathematical Statistics*, 2nd ed, Springer Texts in Statistics (Springer, 2003).
29. E. L. Lehmann and J. P. Romano, *Testing Statistical Hypotheses*, 3rd ed, Springer Texts in Statistics (Springer, 2005).